Prediction of uncertainty of 10-coefficient compressor maps for extreme operating conditions

Howard Cheung

Postdoctoral Research Fellow, Ray W. Herrick Laboratories, School of Mechanical Engineering, Purdue University, 177 S. Russell St., West Lafayette, IN 47907-2031, US

E-mail: cheung@purdue.edu

Christian K. Bach

Assistant Professor, Mechanical and Aerospace Engineering, Oklahoma State University, 218 Engineering North, Stillwater, OK 74078-5016

E-mail: cbach@okstate.edu

Abstract. Empirical compressor maps are a simple and reliable approach for heating and cooling system designers to estimate compressor refrigerant mass flow rate and power consumption quickly. These maps were used for a long time since most compressor manufacturers build the maps with extensive test matrices, leading to good accuracy. However, the situation changes when engineers extrapolate the maps to investigate the compressors performance under extreme operating conditions such as for cold climate heat pump applications or under conditions with system faults. Engineers are not confident on the exact uncertainty of the extrapolation, and often claim that the inaccuracy of their studies is a result of high extrapolation uncertainty. This paper presents a method to estimate the extrapolation uncertainty due to the structure of the test matrix that trains the manufacturer maps and helps the investigators to understand if the extrapolation is the main cause of their inaccuracy. To verify that the method can estimate the uncertainty due to extrapolation, the study builds 10-coefficient compressor maps trained by different test matrices of the same size and different operating points. The maps are used to estimate the compressor performance under different operating points and their estimation uncertainties are compared. The results show that the component of the uncertainty that depends on the structure of the test matrix is small at operating conditions within the test matrix but the uncertainty grows significantly as the estimation becomes further away from the operating conditions within the test matrices.

1. Introduction

Empirical compressor maps for positive displacement compressors, such as the 10-coefficient polynomials outlined in ANSI/AHRI Standard 540 [1] and European Standard EN 12900 [2] are widely used in academia and industry. These maps are trained with experimental data and then used to calculate power input, mass flowrate, current, and compressor efficiency. However, the maps contain squared and cubic terms of the inputs (suction and discharge dew point temperature) and are therefore potentially inaccurate when used at points other than the training data. Manufacturers often state an accuracy of $\pm 5\%$ for tabulated performance data (e.g. [3] or [4]). This paper shows a method that estimates the resulting uncertainty for the 10 coefficient polynomial at a certain point other than the training data set. This paper does not adress interpolation between different speeds of variable speed compressors. The methodology can be extended to predict the uncertainty of the outputs for interpolating between fixed speeds rather than using different fixed speed compressor maps as done by e.g. [5] and [6].

2. Linear regression

Finding the coefficients of the 10 coefficient maps can be treated as a liniear regression problem, whith the evaporation and condensing temperature and their linear, squared and cubed combinations being the independent variables $\vec{x}$ and the power consumption of the compressor being the estimated dependend variable y. To better understand the uncertainty sources of the model, a brief review of linear regression along with how this applies to the polynomial compressor map is shown subsequently.

2.1. Review

Linear regression is used to estimate the parameters of a linear model. Measurement data always includes error, therefore only an estimate of the true parameters can be obtained. If we had the true model parameters $\vec{\beta}_{true}$, then we could use the independent inputs to our model ($\vec{x}^T$) to calculate the true output y_{true} up to an error ε caused by measurement error,

$$y_{true} = \vec{x}^T \vec{\beta}_{true} + \varepsilon. \tag{1}$$

Unfortunately it is not possible to obtain the true model, since all measurement data that is used for training the model has measurement error. Therefore, we need to estimate the model parameters to be able to calculate an estimate of the output. To emphasize the difference between the two models, a hat ($\hat{}$) is used for both, estimated parameters $\hat{\vec{\beta}}$ and estimated output, $\hat{y}$,

$$\hat{y} = \vec{x}^T \hat{\vec{\beta}}. \tag{2}$$

The parameters for the model can be estimated using measuremnt data, for non-weighted reduction of the squares of the errrors it can be shown that the parmeter vector $\hat{\vec{\beta}}$ can be calculated as

$$\hat{\vec{\beta}} = (\mathbf{X}_{train}^T \mathbf{X}_{train})^{-1} \mathbf{X}_{train}^T \vec{y}_{train}, \tag{3}$$

where the training data input matrix $\mathbf{X}_{train}$, composed of input data vectors $\vec{x}_{train,i}$ for each data point i is constructed as

$$\mathbf{X}_{train} = \begin{bmatrix} \vec{x}_{train,1} & \cdots & \vec{x}_{train,i} & \cdots & \vec{x}_{train,n} \end{bmatrix}^T, \tag{4}$$

where n is the total number of data points. The output training data vector is composed of output values $y_{train,i}$ for each data point as

$$\vec{y}_{train} = \begin{bmatrix} y_{train,1} & \cdots & y_{train,i} & \cdots & y_{train,n} \end{bmatrix}^T. \tag{5}$$

The accuracy σ of the model for the training data points is

$$\sigma = \sqrt{\frac{\Sigma_i (y_{train,i} - \vec{x}^T \hat{\vec{\beta}})^2}{n-1}}. \tag{6}$$

2.2. Polynomial compressor map as linear regression problem

ANSI/AHRI Standard 540 [1] estimates the compressor power consumption $\hat{\dot{W}}$ as

$$\hat{\dot{W}} = \beta_1 + \beta_2 T_{evap} + \beta_3 T_{cond} + \beta_4 T_{evap}^2 + \beta_5 T_{evap} T_{cond} + \beta_6 T_{cond}^2 + \beta_7 T_{evap}^3 + \beta_8 T_{evap}^2 T_{cond} + \beta_9 T_{evap} T_{cond}^2 + \beta_{10} T_{cond}^3, \tag{7}$$

where β_i are the (estimated) model coefficients and T_{evap}, T_{cond} are the evaporation and condensing dew point temperatures. Referring to eqn. 2, $\hat{\dot{W}}$ takes the place of $\hat{y}$, the vector composed of β_i is $\hat{\vec{\beta}}$, and the vector of independent variables, $\vec{x}$ is the vector of the independent variables (here: dew point temperatures),

$$\vec{x} = \begin{bmatrix} 1 & T_{evap} & T_{cond} & T_{evap}^2 & T_{evap}T_{cond} & T_{cond}^2 & T_{evap}^3 & T_{evap}^2 T_{cond} & T_{evap} T_{cond} & T_{cond}^3 \end{bmatrix}^T \tag{8}$$

3. Uncertainty of steady state measurements

The training data for compressor maps is obtained from steady state time series data. Steady state time series data does not show any significant monotonic trend in average value but rather shows periodic and random fluctuations (noise) around an average value. The mean value a of the measured variable can be defined as

$$a = \Sigma_{i=1}^{N} \frac{a_{mea}(t_i)}{N}, \tag{9}$$

where $a_{mea}(t_i)$ is a discrete measurement of the variable at time step i, and N is the number of measurements. Measurement devices have an uncertainty which can be considered time independend, often called zero order uncertainty. The limited number of samples in combination with the fluctuations of the variable leads to a second (first order) uncertainty. Zero-order uncertainty is typically provided by the manufacturer of the measurement device, such as $\pm 0.5K$ for T-type thermocouples, or 0.5% of the measured flowrate for Coriolis mass flowmeters. First-order uncertainty is not known in advance but rather needs to be approximated by statistically analyzing the time series data of the steady state measurement. Taylor and Kuyatt (1994)**??** give the overall measurement uncertainty as

$$\Delta a = \sqrt{\Sigma_{i=1}^{N} \left(\frac{\Delta a_{mea}(t_i)}{N} \right)^2 + \left(\frac{t_{N-1,1-\alpha/2}}{N} \right)^2 \frac{\Sigma_{i=1}^{N} (a_{mea}(t_i) - a)^2}{N-1}} \tag{10}$$

where $t_{N-1,1-\alpha}$ is the statistic of the student t distribution with a degree of freedom of N-1 and level at $1 - \alpha/2$. The first part of the uncertainty is the sum of squares of the zero-order uncertainty of each observation within the steady state measurement. The second part of the uncertainty is given as the confidence interval of the average value at the level of $1 - \alpha/2$. In practice, α is taken as 0.1, and a 95% confidence interval is usually used in the approximation.

4. Generating experimental results of steady state data with uncertainties from compressor map data

For this paper, no real measurement data are taken for training data, and only ideal compressor performance data from the manufacturers without uncertainty is available. In order to test the uncertainty calculation of the compressor map output, some training data is needed. Hence it is necessary to approximate a set of training data with uncertainties from the ideal compressor performance data. If the ideal compressor performance data are the true values of the measurement, its measurement value will be different from its true value because it is subjected to the zero-order uncertainty of the measurement device and the first-order uncertainty of the noise of the measurement environment. Assuming that the uncertainty is the confidence interval of the measurement value at a level of $1 - \alpha/2$ and the measurement value follows a normal distribution with a mean value around the true value of the measurement, the standard deviation of the normal distribution will be given by

$$\sigma_{mea} = \frac{\sqrt{(\Delta a_{zero-order}(a = a_{true}))^2 + (\Delta a_{first-order}(a = a_{true}))^2}}{z_{1-\alpha/2}} \tag{11}$$

where $z_{1-\alpha/2}$ is the z-normal distribution statistics given at a level of $1 - \alpha/2$. The observations within steady state can then be approximated by running a random number generator following a normal distribution with mean at the true value of a and standard deviation at mea multiple times. These values can then be analyzed with the method listed in the section 3 to calculate the value and uncertainty of steady state measurement.

5. Sources of uncertainty

Uncertainty of the compressor map output is the range where the true value of the map output may be relative to the map output. It consists of multiple components and can be grouped as follows:

- Uncertainty due to inputs
- Uncertainty due to training data
- Uncertainty due ot model random error
- Uncertainty due to outputs

5.1. Uncertainty due to inputs

Uncertainty due to inputs is the uncertainty propagated to the map output due to the uncertainty in the inputs to the maps. The inputs to the map (evaporating and condenser temperature) are usually obtained by converting pressure measurement to saturation temperature with refrigerant equations of state, and the estimated saturation temperature contains uncertainty from both the equation of state and the pressure measurement. The equation of state of R22 estimates saturation pressure at an uncertainty of 0.2% [7]. When the equation of state estimates an saturation temperature at a given pressure, this uncertainty is transformed into a component of the uncertainty of the saturation temperature as shown in Eqns. (12) and (13).

$$\frac{\Delta P_{sat,EOS}}{P_{sat}(T)} = 0.002 \tag{12}$$

$$\Delta T_{sat,EOS} = |\frac{\partial T_{sat}(P)}{\partial P}|\Delta P_{sat,EOS} \tag{13}$$

where $\Delta P_{sat,EOS}$ is the uncertainty of saturation pressure as a result of uncertainty of the equation of state, $P_{sat}(T)$ is the saturation pressure from temperature T, $\Delta T_{sat,EOS}$ is the uncertainty of saturation temperature as a result of uncertainty of the equation of state and $T_{sat}(P)$ is the saturation temperature at pressure P.

The component of the uncertainty due to pressure measurement in saturation temperature values is calculated by Eqn. (14).

$$\Delta T_{sat,mea} = |\frac{\partial T_{sat}(P)}{\partial P}|\Delta P_{sat,mea} \tag{14}$$

where $\Delta T_{sat,mea}$ is the uncertainty of saturation temperature as a result of pressure measurement and $\Delta P_{sat,mea}$ is the uncertainty of pressure measurement.

The overall uncertainty of the saturation temperature is given by Eqn. (15).

$$\Delta T_{sat} = \sqrt{(\Delta T_{sat,EOS})^2 + (\Delta T_{sat,mea})^2} \tag{15}$$

The uncertainty of the map output propagated from the inputs of condensing temperature and evaporating temperature can be given by Eqn. (16).

$$\Delta \hat{\dot{W}}_{input} = \sqrt{(\frac{\partial \hat{\dot{W}}}{\partial T_{evap}} \Delta T_{evap})^2 + (\frac{\partial \hat{\dot{W}}}{\partial T_{cond}} \Delta T_{cond})^2} \tag{16}$$

where $\Delta \hat{\dot{W}}_{input}$ is the uncertainty due to inputs at the map output

5.2. Uncertainty due to training data

Uncertainty due to training data is the uncertainty propagated to the map output from the training data through the map coefficients. This can be understood by considering the estimation of the map coefficients as a function of the training data as Eqn. (17).

$$\hat{\vec{\beta}} = g(T_{evap,train,1}, ..., T_{evap,train,n}, T_{cond,train,1}, ..., T_{cond,train,n}, \dot{W}_{train,1}, ..., \dot{W}_{train,n}) \tag{17}$$

The uncertainty propagated to the map output through function g and $\hat{\vec{\beta}}$ in Eqn. (17) is calculated by Eqn. (18).

$$\Delta \hat{\dot{W}}_{train} = \sqrt{\begin{aligned} &\Sigma_{j=1}^{n}(\Sigma_{i=1}^{m}(\frac{\partial \hat{\dot{W}}}{\partial \beta_i}\frac{\partial \beta_i}{\partial T_{evap,train,j}})\Delta T_{evap,train,j})^2 \\ &+\Sigma_{j=1}^{n}(\Sigma_{i=1}^{m}(\frac{\partial \hat{\dot{W}}}{\partial \beta_i}\frac{\partial \beta_i}{\partial T_{cond,train,j}})\Delta T_{cond,train,j})^2 \\ &+\Sigma_{j=1}^{n}(\Sigma_{i=1}^{m}(\frac{\partial \hat{\dot{W}}}{\partial \beta_i}\frac{\partial \beta_i}{\partial \dot{W}_{,train,j}})\Delta \dot{W}_{train,j})^2 \end{aligned}} \tag{18}$$

where $\Delta \hat{\dot{W}}_{train}$ is the uncertainty due to training data at the map output

6. Results and discussion

To study how the calculation of compressor map output uncertainty helps to determine the applicability of the map, the performance data of a $4.5kW$ R22 reciprocating compressor listed in its manufacturers specification is used. The tabulated performance data shows the compressor power consumption at different evaporating and condensing temperature with a constant suction superheat 11 K within its operating range as shown in figure 1.

Since the manufacturer data do not include experimental uncertainty, it is assumed that the data in the specification are the true values of the performance, and they are used to approximate the observations during steady state experiments with the assumptions in Table 1.

The steady state experiment is assumed to have been conducted for 10 minutes with data acquired at 0.1Hz. The experimental observations at all data points in Figure 1 are generated by the method listed in section 4.

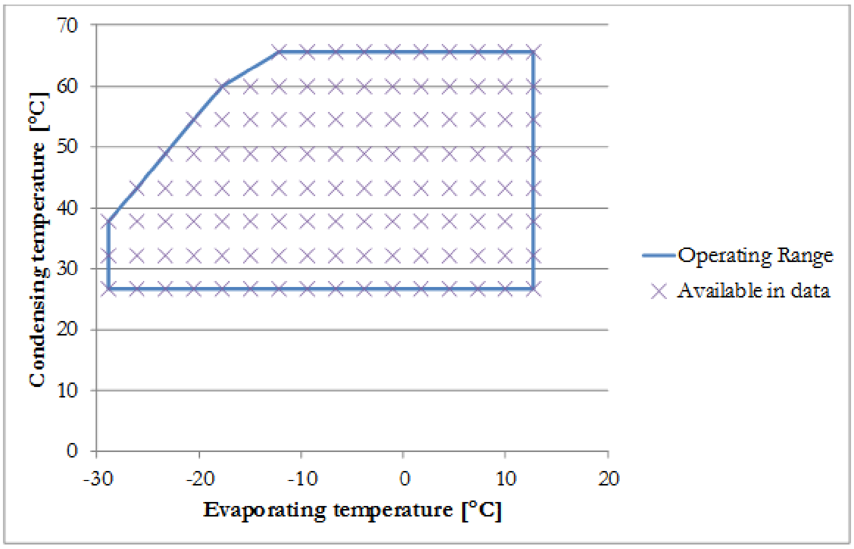

Figure 1. Operating envelope of compressor chosen for this study and available data points from manufacturer map.

Table 1. Assumptions to approximate results in experiments of steady state compressor operation

Variable	Zero-order uncertainty	First-order uncertainty
Power consumption	0.50%	3%
Evaporating pressure	0.80%	0.9kPa
Condensing pressure	0.80%	0.4kPa

6.1. Study cases

To examine if the applicability of compressor map changes with the conditions of the training data, various compressor maps trained from different ranges of data are compared. Six maps with different ranges of training data are designed for the study and the ranges of the training data in these maps are shown in Figure 2.

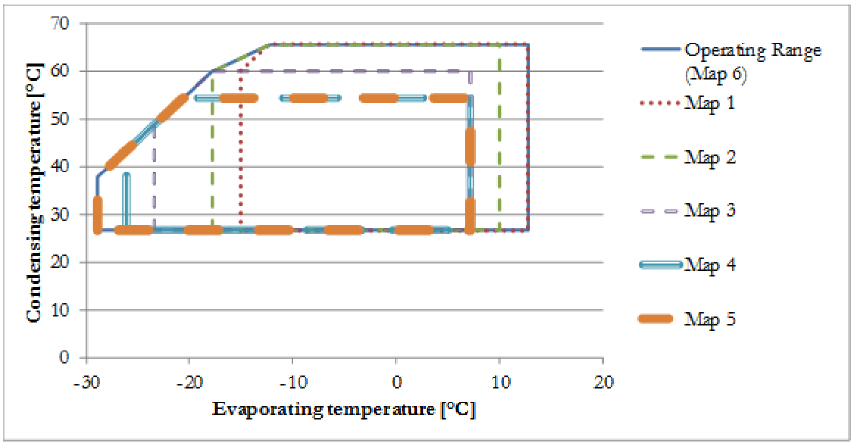

Figure 2. Range of training data for different maps.

Figure 2 shows that map 1 to 5 have their ranges of training data shifting from the top right-handed corner of the operating range of the compressor to its bottom left-handed corner, and map 6 covers the entire operating range. Since it is unfair to compare maps that are generated by different number of data points, the training data points in each map are arranged such that each map contains 70 data points, and the details of the data points in each map can be found in the appendix.

6.2. Comparison of maps

References

[1] Ansi/ahri standard 540: 2004 standard for performance rating of positive displacement refrigerant compressors and compressor units

[2] En 12900:2013. refrigerant compressors - rating conditions, tolerances and presentation of manufacturer's performance data

[3] Technologies E C 2006 Copeland cf and cs compressors 50 hertz - the final solution for hfc performancecopeland cf and cs compressors 50 hertz - the final solution for hfc performance Tech. rep. Sidney, Ohio

[4] Inc B C I 2015 Performance table for h82b343abc Tech. rep.

[5] Bo Shen Omar Abdelaziz C K R 2014 Compressor selection and equipment sizing for cold climate heat pumps *2014 IEA HP conference*

[6] Stephen L Caskey Derek Kultgen E A G W H T M 2012 Simulation of an air-source heat pump with two-stage compression and economizing for cold climates

[7] N T B and E K C 1995 *NIST Technical Note* (Gaithersburg: National Institute of Standards and Technology)